© **2006** Nonlinear Phenomena in Complex Systems

On cytoskeletal patterns and intrinsic disorder effects

Falko Ziebert[1], Martin Hammele[1,2] and Walter Zimmermann[1]

[1] *Theoretical Physics, University of Bayreuth, D-95440, Bayreuth, Germany*
E-mail: Falko.Ziebert@uni-bayreuth.de, Walter.Zimmermann@uni-bayreuth.de
[2] *Theoretical Physics, University of the Saarland, D-66041, Saarbrücken, Germany*
E-mail: maham@lusi.uni-sb.de

(Received ... 2006)

In a model for polar filaments, which are transported relative to each other by molecular motors, the homogeneous and isotropic filament distribution may become either unstable with respect to a stationary or oscillatory orientational instability of finite wavelength or with respect to a density instability, where the small wave numbers are not damped. Beyond these instabilities, in the weakly nonlinear regime, we find a competition between stripe patterns and asters where the asters are preferred in a larger parameter range. Besides the dynamic interactions via motors, filaments may also be connected persistently by crosslinker proteins like actinin. Clusters of permanently linked filaments are likely to be randomly distributed in space and such clusters are expected to affect the formation of patterns. As analyzed here in a simple case, the bifurcation is affected by the disorder in such a way that the onset of patterns becomes more likely, for instance by a reduction of the bifurcation threshold.

Key words: Pattern formation, Subcellular structure and processes, Complex systems, Disorder

PACS numbers: 47.54.+r; 87.16.-b; 89.75.-k; 71.55.-i

1 Introduction

Biological cells are apart from highly specialized biological units like the cell nucleus, mitochondria and other organelles made of a complex fluid, the so-called cytosol. Its main constituents are the cytoskeletal proteins. Most of them are polymerized to actin filaments and microtubules, major parts of the cytoskeleton which is the scaffold of most eukaryotic cells, stabilizes the cell morphology and determines predominantly the mechanical properties of the cell [1]. Apart from this obvious importance for the overall cell structure the cell is organized vastly by an efficient machinery which involves in addition to the cytoskeletal polymers also different kinds of associated proteins like motor proteins [2], crosslinkers, capping proteins etc. Motors are specialized proteins that can move on the polymer scaffold either to perform intracellular transport or to organize actively the cytoskeleton if in contact with several filaments.

The elastic properties of the cytoskeleton have attracted recently a huge activity from physical sciences [3]. A similiar trend can be observed for the nonequilibrium processes in cells. In a living cell the various types of polymerization and depolymerization processes of cytoskeletal filaments and the motor-mediated transport which both need the chemical fuel ATP (Adenosine triphosphate) are interesting nonequilibrium processes. A number of these processes are related to elementary questions on dissipative pattern formation in cellular materials [4, 5, 6], and to what extent they are involved in the cellular organization.

In early experiments, motor-filament systems have been studied in contractile filament bundles [7, 8, 9] similar as in muscles. Later, motivated by similarities to biologically relevant structures like e.g. the mitotic spindle, pattern formation in quasi two-dimensional dilute motor-filament solutions was investigated and a huge variety of patterns like bundles, asters, vortices and more complicated

structures have been found [10, 11]. Phenomenological [12] and mesoscopic [13, 14, 15] modeling efforts for such solutions have been published quite recently.

However, describing a complex fluid like the cytoskeleton by a mean field-like approach - as all theoretic efforts do so far apart from the MD simulations in Ref. [11] - neglects the inherent presence of disorder as it obviously occurs in biological cells: besides the dynamic filament interaction via the motor proteins, actin filaments may also be linked quasi permanently by crosslinker proteins, e.g. α-actinin, filamin, fimbrin etc. [1]. Such crosslinkers are used by the cell in quite high concentrations to form gels, e.g. the cell cortex underneath the membrane. In vitro these actin-linking proteins lead in high concentrations to networks of semiflexible polymers which are in the focus of a number of mechanical investigations [16, 17]. However, even after several purification procedures usually performed to get an actin solution for in vitro experiments, it is very likely that always a small amount of such linking proteins remains in the actin solution. Such small fractions of linking proteins may cause small clusters of actin filaments, such clusters being rather immobile as compared to single filaments. Since the oligomeric motor proteins can still bind to such clusters, single filaments may still undergo motor transport relative to these clusters. Therefore the crosslinked clusters represent a realization of a frozen disorder in the cytoskeleton problem.

At least what pattern formation is concerned, the influence of disorder may change a bifurcation from a spatially homogeneous state to a spatially periodic state considerably, as was studied and established for models of pattern formation in hydrodynamic [18, 19, 20, 21] and chemical systems [22, 23]. In those examples as well as for cytoskeletal patterns, the onset of pattern formation is reduced by the disorder as we desribe in Sec. 5.

The text is organized as follows: first a mesoscopic model for a filament-motor system is described. Upon coarse graining, one gets evolution equations for the density and orientation field of the filaments, which should be sufficient to describe the system in the dilute and semi-dilute regime. Then the possible pattern forming instabilities are extracted and a generic description via amplitude equations is sketched. In the last part, the effect of parametric disorder is briefly discussed in the framework of the amplitude equation of the stationary bifurcation.

2 A mesoscopic model for filament-motor systems

Our starting point is the probability distribution function $\Psi(\mathbf{r},\mathbf{u},t)$ for filaments, where the filament orientation is described by a unit vector $\mathbf{u}$. The dynamics of $\Psi(\mathbf{r},\mathbf{u},t)$ is governed by the Smoluchowski equation for rigid rods [15]

$$\partial_t \Psi + \nabla \cdot \mathbf{J}_t + \mathcal{R} \cdot \mathbf{J}_r = 0 \quad , \tag{1}$$

which is also called the Doi equation [24]. This equation just describes the conservation of the probability. For a solution of rods, one has the divergence of a translational current, $\mathbf{J}_t$, and a rotational current, $\mathbf{J}_r$, which enters into Eq. (1) with the rotational operator $\mathcal{R} = \mathbf{u} \times \partial_{\mathbf{u}}$, the analogon of the ∇-operator on the unit sphere. The translational and rotational currents can be written in the following form

$$J_{t,i} = -D_{ij}\left[\partial_j \Psi + \Psi \partial_j V_{ex}\right] + J^a_{t,i} \ , \tag{2}$$

$$J_{r,i} = -D_r\left[\mathcal{R}_i \Psi + \Psi \mathcal{R}_i V_{ex}\right] + J^a_{r,i} \ , \tag{3}$$

with an uniaxial diffusion matrix D_{ij} and a rotational diffusion coefficient D_r governing the rotational Brownian motion. The excluded volume effect generated by neighboring filaments is described by the potential V_{ex}

$$V_{ex}(\mathbf{r},\mathbf{u}) = \int d\mathbf{u}' \int d\mathbf{r}' \; W(\mathbf{r}-\mathbf{r}',\mathbf{u},\mathbf{u}')\Psi(\mathbf{r}',\mathbf{u}'), \tag{4}$$

similar as in Onsager's theory of the isotropic-tonematic (I-N) transition [25]. The interaction kernel W is assumed to be unity if the two filaments at $(\mathbf{r},\mathbf{u})$ and $(\mathbf{r}',\mathbf{u}')$ overlap and it vanishes otherwise.

In the absence of the active currents $\mathbf{J}^a_t$ and $\mathbf{J}^a_r$ the system of Eqs. (1)-(4) describes the diffusive motion of rods that interact via the excluded volume effect and this case is discussed extensively, for

instance, in Ref. [24]. The active filament currents are induced by the action of molecular motors that consume energy via the hydrolysis of ATP. If one assumes that a motor binds preferentially at an angle smaller than $\pi/2$ as has been assumed in [13], the rotational contribution $\mathbf{J}_r^a$ is purely nonlinear. Its behavior on pattern selection was discussed to some extent in [15] but for reasons of simplicity we neglect this contribution here, i.e. $\mathbf{J}_r^a = 0$. If one assumes only two-filament-interactions, which is reasonable in the dilute limit, one can write

$$\mathbf{J}_t^a = \Psi(\mathbf{r},\mathbf{u})\int d\mathbf{u}'\int d\mathbf{r}'\ \mathbf{v}\ W(\mathbf{r}-\mathbf{r}',\mathbf{u},\mathbf{u}')\Psi(\mathbf{r}',\mathbf{u}'). \quad (5)$$

This current describes the action of an oligomer of molecular motors that sets two filaments at $(\mathbf{r},\mathbf{u})$ and $(\mathbf{r}',\mathbf{u}')$ into relative motion if it is in contact with both filaments. Such a simultaneous contact is again described by the overlap function W in Eq. (5) and the induced velocity $\mathbf{v}$ is described below.

The motor density here is assumed to be large so that there are always motors around to induce a relative filament motion if the overlap integral in Eq. (5) becomes finite. The actively generated relative filament velocity $\mathbf{v}$ depends on the relative separation of the center of masses of the rods as well as on the orientation of the rods

$$\mathbf{v}(\mathbf{r},\mathbf{r}',\mathbf{u},\mathbf{u}') = \mathbf{v}(\mathbf{r}-\mathbf{r}',\mathbf{u},\mathbf{u}')\ . \quad (6)$$

By symmetry considerations [13], the translational velocity can be represented in leading order by

$$\mathbf{v}(\mathbf{r},\mathbf{r}',\mathbf{u},\mathbf{u}')=\frac{\alpha(\mathbf{r}-\mathbf{r}')}{2L}\frac{1+\mathbf{u}\cdot\mathbf{u}'}{|\mathbf{u}\times\mathbf{u}'|}+\frac{\beta}{2}\frac{\mathbf{u}'-\mathbf{u}}{|\mathbf{u}\times\mathbf{u}'|}. \quad (7)$$

The coefficients α and β are macroscopic and phenomenological transport coefficients for the complex processes at the length scale of molecular motors. By restricting the filament motion to one spatial dimension and the filament orientation also to this direction, then α and β correspond to the relative transport of parallel and anti-parallel filaments respectively, as can be seen by comparing this model with a model for filament bundling [26].

2.1 Coarse grained equations for the first two moments.

According to the excluded volume interaction and the active currents $\mathbf{J}_t$ and $\mathbf{J}_r$ the system of Eqs. (1)-(4) is nonlocal and nonlinear with a quadratic contribution $\propto \Psi^2$. If the spatial variations of $\Psi(\mathbf{r},\mathbf{u},t)$ are small on the length scale of filaments the nonlocal interaction may be removed by a gradient expansion of the integral kernel in Eqs. (4) and (5). A moment expansion similar as performed in Ref. [27] close to the I-N transition here leads to two coupled evolution equations for the coarse grained density of the filaments

$$\rho(\mathbf{r},t) \ = \ \int d\mathbf{u}\ \Psi(\mathbf{r},\mathbf{u},t)\ , \quad (8)$$

and the orientation field

$$\mathbf{t}(\mathbf{r},t) \ = \ \int d\mathbf{u}\ \mathbf{u}\ \Psi(\mathbf{r},\mathbf{u},t)\ . \quad (9)$$

The coupled equations for the two moments are given in the appendix, their derivation can be found in [15]. It is important to notice that the orientation field is a vector field and not a director field as in nematic liquid crystals. Since motor proteins move according to the helical structure of the actin filaments or the microbutules always in one direction, the $\pm\mathbf{u}$-symmetry is broken and the vector field $\mathbf{t}$ is a relevant quantity in a filament-motor system. However, also lyotropic nematic order may occur in densely packed actin filaments and microtubules [28, 29]. Nevertheless, in the presence of motors the polar orientation will often dominate because the vector field $\mathbf{t}(\mathbf{r},t)$ becomes already important far below the critical density of the isotropic-nematic transition [15].

3 Pattern forming instabilities

A homogeneous filament density, as described by a constant ρ_0, with isotropically distributed filament-orientation, i.e. $\mathbf{t} = 0$, will be referred to as the basic state. This basic state may become unstable with respect to a pattern forming instability, if the filament density ρ_0 or the motor activity parameter α is increased beyond some critical values [14, 15]. With $\tilde{\rho}$ we describe the deviations

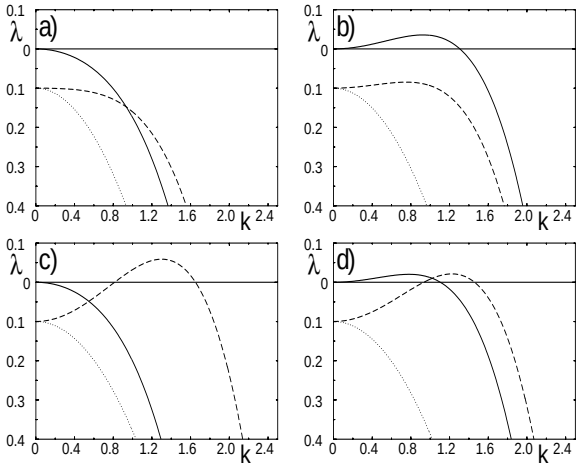

FIG. 1. The growth rates in the stationary case $\beta = 0$, where $\sigma = \mathrm{Re}[\sigma(k)] = \lambda$. The eigenvalue σ_d corresponding to the instability with respect to density fluctuations (solid line) as well as the one with respect to orientational fluctuations, σ_L (dashed line), are shown as a function of the wave number k for $D_r = 0.1$. The third eigenvalue σ_T is dampened as depicted by the dotted line. Parameters are a) $\alpha = 25$, $\rho_0 = 1.1$ leading to a linearly stable state; b) $\alpha = 35$, $\rho_0 = 0.85$ leading to a density instability; c) $\alpha = 20$, $\rho_0 = 1.7$ leading to an orientational instability; d) $\alpha = 28$, $\rho_0 = 1.185$ both density and orientational fluctuations are unstable.

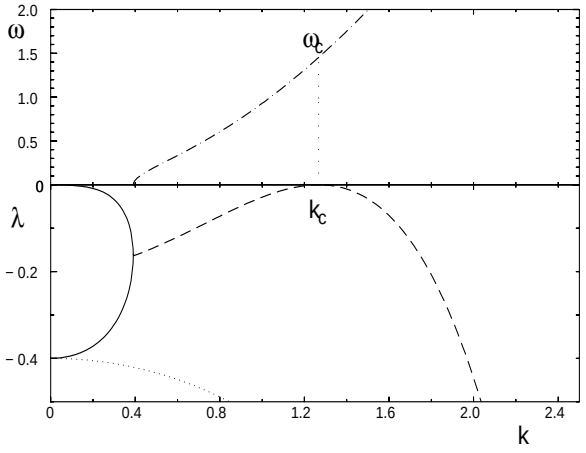

FIG. 2. The case with finite β. The real part λ and the imaginary part ω of the growth rate are shown in dependence of wave number k as the dashed and dash-dotted line respectively. At the point where the density and the longitudinal orientation branch meet, the growth rate gains a non-vanishing imaginary part, i.e. the instability becomes oscillatory. Parameters are $\alpha = 17$, $\beta = 3$, $D_r = 0.4$ and $\rho = \rho_\beta$.

of the filament density from the basic state with $\rho(\mathbf{r}, t) = \rho_0 + \tilde{\rho}(\mathbf{r}, t)$.

The critical values for the density and α are determined by linearizing the basic equations, as given by Eqs. (18), with respect to small deviations $\tilde{\rho}$ and $\mathbf{t}$ from the basic state. The resulting three (in two spatial dimensions) coupled linear partial differential equations, written in vectorial form by introducing $\mathbf{w} = (\tilde{\rho}, t_x, t_y)$, read

$$\partial_t \mathbf{w}(\mathbf{r}, t) = \mathcal{L}_0 \mathbf{w}(\mathbf{r}, t)\,. \tag{10}$$

These equations have constant coefficients and by a Fourier transformation one obtains an eigenvalue problem with three different eigenvalues $\sigma_l(k) = \lambda_l(k) + i\omega_l(k)$ $(l = 1, 2, 3)$.

For $\beta = 0$ the eigenvalues are real and their wave number dependence is shown for different parameter sets in Fig. 1. One can identify a density mode (solid line), a longitudinal orientation mode (dashed line) and a transversal orientation mode (dotted line). For the parameter set used in Fig. 1a) the basic state is stable and in part b) the basic state becomes unstable with respect to a density instability. The dispersion $\lambda(k)$ as described by the solid curve in Fig. 1b) is typical for instabilities where a conservation law is involved as it is the case in our system for the overall amount of filaments. The dashed curve in Fig. 1c) is an instability with finite wavelength which corresponds in our model to a longitudinal orientational instability, i.e. the wave number $\mathbf{k}$ and the orientational field $\mathbf{t}$ have the same direction. Part d) of Fig. 1 shows the case, where the basic state becomes unstable with respect to both, a density instability and an orientational instability. This may lead to complex nonlinear interaction phenomena, as discussed elesewhere. The transverse orientation mode is always dampened, as shown by the dotted lines in Fig. 1.

The presence of a non-vanishing parameter β leads to a qualitative change of the instabilities. While in the case $\beta = 0$ all the eigenvalues are real, the eigenvalues of the density and the longitudinal orientation merge in the case $\beta \neq 0$ and one obtains

a complex conjugate pair of eigenvalues (Hopf bifurcation) with a maximum at finite values of the wave number, as shown in Fig. 2. As in the case $\beta = 0$, also the (real and conserved) long wavelength mode can become unstable and the interaction with the finite wave number Hopf instability again leads to interesting phenomena as discussed elsewhere.

The critical filament densities for the above instabilities can easily be calculated. Its value for the long wavelength density instability is given by

$$\rho_d = \frac{1}{\frac{\alpha}{18} - \frac{2}{\pi}}, \tag{11}$$

providing that this value is positive, i.e. if $\alpha > \frac{36}{\pi}$ holds. Otherwise the density instability is impossible. One should note that ρ_d is independent of β since the coupling of the density and the orientation mode through the β-terms is $\mathcal{O}(k^4)$ and the instability is determined by the change of sign of $\partial_k^2 \sigma_d$.

The finite wave number longitudinal orientational mode gets unstable for a filament density exceeding

$$\rho_\alpha = \frac{8}{\alpha}\left(\frac{7}{2} + \frac{5}{12} D_r \left(1 + \sqrt{1 + \frac{84}{5 D_r}}\right)\right) \tag{12}$$

in the case $\beta = 0$. For finite β one gets the critical density ρ_β as the solution of the quadratic equation

$$\frac{151}{11520} D_r \alpha \rho_\beta = \left[\left(\frac{7\alpha}{96} - \frac{3}{2\pi}\right)\rho_\beta - \frac{13}{8}\right]^2 . \tag{13}$$

One should note that ρ_β does not depend on β since the β-contributions are off-diagonal and therefore only influence the frequency of the oscillatory instability.

The critical wave numbers k_c^α and k_c^β respectively and the frequency ω_c in the case $\beta \neq 0$ can also be easily obtained [15, 33].

4 Weakly nonlinear description of patterns

For values of the control parameter, here the mean filament density ρ_0, near the threshold of a supercritical bifurcation with a finite wave number, an amplitude expansion can be performed to describe the dynamics of the pattern on slow time scales and for small modulations of the spatially periodic pattern [4].

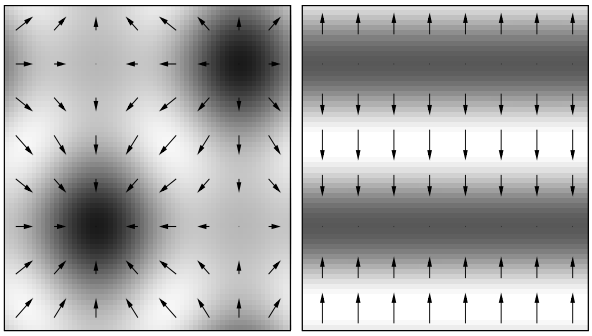

FIG. 3. Numerically obtained stationary nonlinear solutions of the investigated model as they are also described by the simple amplitude equations for orthogonal rolls, Eqs. (15). On the left a square pattern where the pattern implied by the orientation field (the arrows) strongly resembles patterns, so-called asters, in *in vitro* experiments of microtubules and motors [11]. The density field is color-coded with white color as high and dark color as low density. On the right the stripe pattern, which can also be obtained in the orthogonal direction.

In the stationary case, i.e. $\beta = 0$, the generic patterns in two–dimensional systems close to threshold are stripes, squares or hexagonal patterns. From both the hierarchy of equations that has to be solved during the derivation of the amplitude equations and from numerical simulations of the full underlying equations, hexagons can be discarded and the only possible solutions are stripes in two orthogonal directions [15]. The generic equations for the amplitudes A and B of the critical modes,

$$\begin{pmatrix} \rho \\ t_x \\ t_y \end{pmatrix} = \begin{pmatrix} 0 \\ A \\ 0 \end{pmatrix} e^{ik_c^\alpha x} + \begin{pmatrix} 0 \\ 0 \\ B \end{pmatrix} e^{ik_c^\alpha y} + c.c. \tag{14}$$

(c.c. describes the complex conjugate) then read

$$\begin{aligned} \tau_0 \partial_t A &= \varepsilon A - \left(g_1 |A|^2 + g_2 |B|^2\right) A \ , \\ \tau_0 \partial_t B &= \varepsilon B - \left(g_1 |B|^2 + g_2 |A|^2\right) B \ , \end{aligned} \tag{15}$$

reflecting the possibility of roll patterns in $x-$ and $y-$directions and its superposition as a square pattern. Here $\varepsilon = \frac{\rho_0 - \rho_\alpha}{\rho_\alpha}$ is the deviation from the

threshold of the stationary longitudinal orientation mode. τ_0, g_1 and g_2 are coefficients that link the generic amplitude equation to the specific underlying model system. The stationary nontrivial solutions of Eqs. (15) are shown in Fig. 3. For small deviations from the threshold, they agree with the full numerical solution of Eqs. (18,19) [15].

For $\beta \neq 0$ and close to the Hopf bifurcation one can derive from the basic Eqs. (18,19) restriced to one spatial dimension two coupled equations for the amplitudes of a left and a right traveling wave, similar as described in detail in other systems [4, 30]. In two spatial dimensions one obtains a set of four coupled equations for the left and right traveling waves along the two spatial directions, which show interesting nonlinear couplings [31, 32]. The derivation and detailed analysis of the respective equations, which allows for interesting solutions like traveling and breathing asters, is described in detail in Ref. [33].

5 Influence of inhomogeneities on pattern formation

Our models so far were based on the assumption that filaments are only temporarily and dynamically linked by motor proteins. The macroscopic description led to *ideal* patterns like stripes or asters in the stationary case [15] and traveling waves in the oscillatory case.

However, in the cell cortex for instance, actin filaments may also be linked nearly permanently by proteins such as α-actinin, filamin, fimbrin etc. [1] to form gel-like or network-like structures. The presence of a high concentration of these crosslinking proteins leads to a semiflexible elastomer.

In the opposite limit, if the crosslinker density is too small for the system to percolate and build up a gel or network, such a small amount of crosslinkers may cause randomly distributed small clusters of several filaments. The motors still walk on such clusters, transporting single filaments from the solution, thus the clusters represent a noise in the problem. Since these clusters diffuse much slower than single filaments (diffusion scales with mass), if at all, they represent a time independent, frozen random contribution to the mean density ρ_0.

Additionally, there is a much higher probability that an oligomeric motor protein hits such a cluster than a single filament. So single filaments may be transported with a higher efficiency with respect to clusters than with respect to single filaments. Therefore also the effective motor transport parameters α and β may adapt different values close to such a cluster than close to a single filament.

To conclude, randomly distributed clusters cause a frozen random contribution to the mean density ρ_0 as well as to the motor parameters. Close to the onset of spatially periodic patterns the dynamics of the amplitude of the patterns may be described by amplitude equations as was exemplified for the cytoskeleton model in section 4. If we assume a small magnitude of the random contribution, the major effects of the randomness should be taken into account close to the bifurcation point by the respective amplitude equations.

For simplicity, we discuss here only the case of a stationary supercritical (i.e. forward) bifurcation, where rich behaviour can already be expected. In the amplitude equation for such a pattern, that is spatially periodic only in one direction for simplicity (consider e.g. the stripe solution of Eq. (15)) the randomness may cause different contributions: a frozen randomness destroys for instance the translational invariance and therefore allows for quadratic contributions in the amplitude. Without being complete, the amplitude equation can have the following possible random contributions $\xi(x)$, $\xi_2(x)$ and $\xi_3(x)$:

$$\begin{aligned} \tau_0 \partial_t A &= (\varepsilon + \xi(x) + \lambda^2 \partial_x^2) A + \xi_2(x) f(A^2, |A|^2) \\ &\quad - g_1 |A|^2 A + \xi_3(x) \ . \end{aligned} \tag{16}$$

As compared to Eq. (15), we have allowed for slow spatial variations of the amplitude with a coherence length λ [4], which can also be derived straightforwardly from the underlying model. $\xi(x)$ is a multiplicative noise, $\xi_3(x)$ is an additive noise and $\xi_2(x)$ is a term coupling to the square of the amplitude. Which of these contributions is most important depends on the system and the underlying model that has been used.

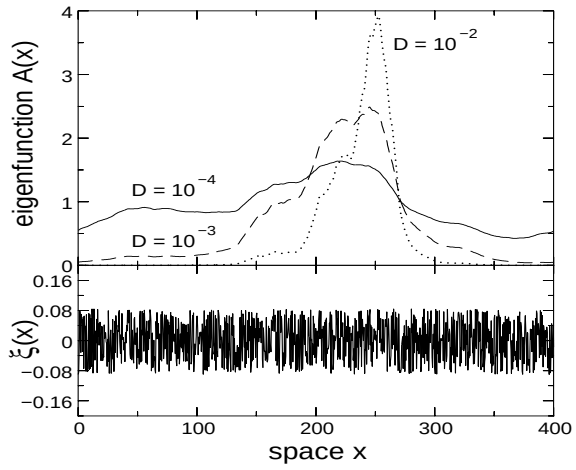

FIG. 4. The spatial structure of the eigenfunction of the linear part $[\varepsilon + \xi(x) + \partial_x^2]A = 0$ is displayed for a realization of the noise $\xi(x)$, as shown in the lower part, but for three different noise amplitudes D.

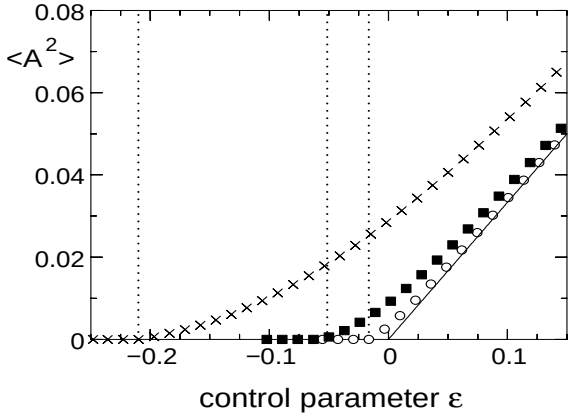

FIG. 5. The averaged squared amplitude $\langle A^2 \rangle$ is shown as a function of the control parameter ε for different values of the noise amplitude: $D = 0.01$ (circles), $D = 0.04$ (squares) and $D = 0.25$ (crosses). The solid line corresponds to the non-disordered case ($D = 0$) where $A^2 = \varepsilon/g$ holds.

Here we just highlight briefly the effect of $\xi(x)$ and choose $\xi_2(x) = \xi_3(x) = 0$. We assume a vanishing mean value $\langle \xi(x) \rangle = 0$ and a delta-correlated second moment

$$\langle \xi(x)\xi(x') \rangle = D\delta(x - x') \tag{17}$$

for the noise [34]. One realization of this parametric disorder is shown in the bottom part in Fig. 4. In the absence of noise, the solutions $A(x)$ are simply constant functions or spatially periodic functions. With noise however, depending on the noise amplitude, $A(x)$ becomes localized as indicated in the upper part of Fig. 4 for the same realization of $\xi(x)$ but for three different amplitudes D. This localization is most strongly pronounced at the threshold and it becomes weaker for larger values of the control parameter.

Second, we find a reduction of the threshold due to such a multiplicative frozen noise, as shown for instance by Fig. 5 for three different values of the noise strength. The curves in Fig. 5 are mean values as obainted by averaging over 100 realizations of the random noise. The threshold values are $< \varepsilon_c >= -1.637 \times 10^{-2}$ for $D = 0.01$, $< \varepsilon_c >= -5.144 \times 10^{-2}$ for $D = 0.04$ and $< \varepsilon_c >= -0.21$ for $D = 0.25$. Besides the reduction of the threshold also the slope of the bifurcation is reduced as shown in Fig. 5.

According to these results for the threshold reduction we expect pattern formation in cytoskeletal solutions to be more likely in the presence of clusters than without disorder. We expect that random effects as described by the noise contributions $\xi_2(x)$ and $\xi_3(x)$ amplify this trend further and make pattern formation possible at even smaller values of the control parameter. A derivation of the noise contributions, as pointed out in Eq. (16), from mesoscopic models like Eqs. (18,19) is required for a further elucidation of these effects.

6 Conclusions and perspective

We have discussed pattern formation in a cytoskeletal solution consisting of filaments (actin or microtubules), motor proteins (e.g. myosin for actin or kinesin in the case of microtubules) and crosslinkers (e.g. actinin). Starting from a mesoscopic model of a filament-motor solution which can be coarse-grained to equations for the density and the orientation of the filaments, one can investigate various instabilities and derive generic amplitude equations for stationary orientational and oscillatory density-orientation patterns. The addition of crosslinkers introduces in the dilute case, due to the formation

of small filament clusters, an inherent parametric disorder into the pattern formation problem.

If this disorder is weak, its effects can be taken into account close to the threshold by the amplitude equations. If the disorder occurs parametrically in the linear part of the equation, disorder reduces the onset of pattern formation considerably. The disorder effects are strong close to the threshold and they become weaker with increasing values of the control parameter as shown in Fig. 5. The localization effect of the amplitude, c.f. Fig. 4, is most strongly pronounced close to the threshold too.

By deriving the amplitude equation in Eq. (16) from mesoscopic models, the relative noise contributions can be interpreted more clearly. Nevertheless, we expect that both contributions $\xi_2(x)$ and $\xi_3(x)$ amplify the tendency to extend the existence of patterns to even smaller values of the control parameter. Recent experiments in actin-myosin systems with very small fractions of streptavidin crosslinkers [35] seem to support the importance of the disorder-induced threshold lowering effect in this very system.

If small and permanently linked clusters increase beyond the percolation threshold one obtains a globally linked filament network. The dynamics that occurs by the interaction of this network with free filaments via the motor action is another interesting and biologically relevant problem to be investigated from the point of views of cell mechanics and self organization.

7 Appendix: Coarse grained equations for density and orientation

The full equations read (with the dot meaning the partial derivative with respect to time and $\mathbf{t} = (t_x, t_y)$ in two dimensions)

$$\begin{aligned}
\dot{\rho} =& \frac{3}{4}\Delta\rho + \left[\frac{3}{2\pi} - \frac{\alpha}{24}\right]\nabla\cdot(\rho\nabla\rho) \\
&- \frac{\alpha}{48}\partial_i\Big[t_i\partial_j t_j + t_j\partial_i t_j + t_j\partial_j t_i\Big] \\
&- \frac{\alpha}{C_1}\Big\{38\nabla\cdot(\rho\nabla\Delta\rho) + 11\partial_i\left(t_j\partial_i\Delta t_j\right) \\
&\quad +16\partial_i\Big[t_i\Delta\partial_l t_l + 2t_l\partial_l\partial_i\partial_l t_l + t_l\partial_l\Delta t_i\Big]\Big\} \\
&- \frac{\beta}{96}\partial_i\Big[\rho\partial_i\partial_j t_j - t_j\partial_j\partial_i\rho + \frac{3}{2}(\rho\Delta t_i - t_i\Delta\rho)\Big], \quad (18)
\end{aligned}$$

$$\begin{aligned}
\dot{t}_i =& -D_r t_i + \frac{5}{8}\Delta t_i + \frac{1}{4}\partial_i\nabla\cdot\mathbf{t} \\
&+ \frac{1}{4\pi}\Big[5\partial_j\left(t_i\partial_j\rho\right) + \partial_j(t_j\partial_i\rho) + \partial_i(t_j\partial_j\rho)\Big] \\
&- \frac{\alpha}{96}\partial_j\Big[3t_i\partial_j\rho + t_j\partial_i\rho + \rho(\partial_i t_j + \partial_j t_i)\Big] \\
&+ \frac{\alpha}{96}\partial_i\Big[t_l\partial_l\rho + \rho\partial_l t_l\Big] - \frac{16\alpha}{C_2}\partial_i\Big[\Delta\partial_l t_l + t_l\partial_l\Delta\rho\Big] \\
&- \frac{\alpha}{C_2}\partial_j\Big[\rho\Big(11\partial_j\Delta t_i + 16\partial_i\Delta t_j + 32\partial_j\partial_i\partial_l t_l\Big) \\
&\quad +16t_j\partial_i\Delta\rho + 32t_l\partial_l\partial_i\partial_j\rho + 44t_i\partial_j\Delta\rho\Big] \\
&+ \frac{\beta}{2}\partial_j\Big[\frac{1}{2}\delta_{ij}\rho^2 - t_i t_j + \frac{1}{48}\Big(\frac{3}{4}\delta_{ij}\rho\Delta\rho + \frac{1}{2}\rho\partial_i\partial_j\rho\Big)\Big] \\
&- \frac{\beta}{96}\partial_j\Big[t_l\partial_l\partial_i t_j + t_i\partial_j\partial_l t_l + t_i\Delta t_j\Big] \ . \quad (19)
\end{aligned}$$

with $C_1 = 23040$ and $C_2 = 2C_1$. Time, space, density and orientation field are written in rescaled units defined by (L the filament length)

$$t' = \frac{D_\parallel}{L^2}t, \ \ x' = \frac{1}{L}x, \ \ \rho\,' = L^2\rho, \ \ \mathbf{t}' = L^2\mathbf{t}. \quad (20)$$

The rescaled diffusion and motor parameters read

$$\begin{aligned}
D_r' &= \frac{L^2}{D_\parallel}D_r \ , \ \ \frac{D_\perp}{D_\parallel} = \frac{1}{2} \ , \\
\alpha' &= \frac{L}{D_\parallel}\alpha \ , \ \ \beta\,' = \frac{L}{D_\parallel}\beta \ , \quad (21)
\end{aligned}$$

where the relation of the translational diffusion coefficients holds for dilute solutions. For a derivation of Eqs. (18,19) we refer to Ref. [15].

References

[1] B. Alberts et. al. *Molecular Biology of the Cell.* (Garland Publishing, New York, 2001).

[2] J. Howard. *Mechanics of Motor Proteins and the Cytoskeleton* (Sinauer, Sunderland, 2001).

[3] A.R. Bausch and K. Kroy. Cytoskeleton from the assembly line: a bottom-up approach to cell mechanics. to appear in Nature Physics.

[4] M. C. Cross and P. C. Hohenberg. Pattern Formation outside of equilibrium. Rev. Mod. Phys. **65**, 851 (1993).

[5] M. Hammele and W. Zimmermann. Modelling oscillatory microtubule polymerization. Phys. Rev. E **67**, 021903 (2003).

[6] F. Ziebert and W. Zimmermann. Pattern formation driven by nematic ordering of assembling biopolymers. Phys. Rev. E **70**, 022902 (2004).

[7] K. Takiguchi. Heavy Meromyosin Induces Sliding Movements between Antiparallel Actin filaments. J. Biochem. **109**, 520 (1991).

[8] H. Nakazawa and K. Sekimoto. Polarity Sorting in a Bundle of Actin filaments by Two-Headed Myosins. J. Physiol. Soc. Japan **65**, 2404 (1996).

[9] A. Ott. The molecular motor actin-myosin on a substrate, in *Transport and Structure*, S. C. Müller, J. Parisi and W. Zimmermann, Eds. (Springer, Berlin, 1999).

[10] R. Urrutia et. al. Purified kinesin promotes vesicle motility and induces active sliding between microtubules in vitro. Proc. Natl. Acad. Sci. USA **88**, 6701 (1991).

[11] F. J. Nedelec, T. Surrey, A. C. Maggs and S. Leibler. Self-organization of microtubules and motors. Nature **389**, 305 (1997).

[12] H. Y. Lee and M. Kardar. Macroscopic equations for pattern formation in mixtures of microtubules and motors. Phys. Rev. E **64**, 056113 (2001).

[13] T. B. Liverpool and M. C. Marchetti. Instabilities of Isotropic Solutions of Active Polar Filaments. Phys. Rev. Lett **90**, 138102 (2003).

[14] F. Ziebert and W. Zimmermann. Comment on "Instabilities of isotropic solutions of active polar filaments". Phys. Rev. Lett. **93**, 159802 (2004).

[15] F. Ziebert and W. Zimmermann. Nonlinear competition between asters and stripes in filament-motor systems. Eur. Phys. J. E **18**, 41 (2005).

[16] D. Humphrey, C. Duggan, D. Saha, D. Smith and J. Käs. Active Fluidization of polymer networks through molecular motors. Nature **416**, 413 (2002).

[17] M.L. Gardel, F. Nakamura, J.H. Hartwig, T.P. Stossel and D.A. Weitz. Prestressed F-actin networks cross-linked by hinged filamins replicate mechanical properties of cells. Proc. Natl. Acad. Sci. USA **103**, 1762 (2006).

[18] W. Zimmermann, M. Seesselberg and F. Petruccione. Effects of disorder in Pattern-Formation. Phys. Rev. E **48**, 2699 (1993).

[19] R. Schmitz and W. Zimmermann. Spatially periodic modulated Rayleigh-Bénard convection. Phys. Rev. E **53**, 5993 (1996).

[20] W. Zimmermann, B. Painter and R. Behringer. Pattern formation in inhomogeneous convective systems. Eur. Phys. J. B **5**, 575 (1998).

[21] M. Hammele, S. Schuler and W. Zimmermann. Effects of parametric disorder on a stationary bifurcation. (to appear in Physica D).

[22] A. Sanz-Anchelergues, A. M. Zhabotinsky, I. R. Epstein and A. P. Munuzuri. Turing pattern formation induced by spatially correlated noise. Phys. Rev. E **63**, 056124 (2001).

[23] R. Peter, et. al. Stripe-hexagon competition in forced pattern-forming systems with broken up-down symmetry. Phys. Rev. E **71**, 046212 (2005).

[24] M. Doi and S.F. Edwards. *The Theory of Polymer Dynamics.* (Clarendon Press, Oxford, 1986).

[25] L. Onsager. The Effects of Shapes on the Interaction of Colloidal Particles. Ann. N.Y. Acad. Sci. **51**, 627 (1949).

[26] K. Kruse and F. Jülicher. Actively contracting bundles of polar filaments. Phys. Rev. Lett. **85**, 1778 (2000).

[27] T. Shimada, M. Doi and K. Okano. Concentration fluctuations of stiff polymers. III. Spinodal decomposition. J. Chem. Phys. **88**, 7181 (1988).

[28] A. L. Hitt, A. R. Cross and R. C. Williams, Jr. Microtubule Solutions Display Nematic Liquid Crystalline Structure. J. Bio. Chem. **265**, 1639 (1990).

[29] A. Suzuki, T. Maeda and T. Ito. Formation of liquid crystalline phase of actin filament solutions and its dependence on filament length as studied by optical birefringence. Biophys. J. **59**, 25 (1991).

[30] W. Schöpf and W. Zimmermann. Convection in binary fluids: Amplitude equations, codimension-2 bifurcation, and thermal fluctuations. Phys. Rev. E **47**, 1739 (1993).

[31] W. Zimmermann. On Traveling Waves in Electrohydrodynamic Convection in Nematics, in *Defects, singularities and patterns in nematic liquid crystals: Mathematical and Physical aspects.* J. M. Coron et. al., Eds. (Kluwer, 1991).

[32] M. Silber, H. Riecke and L. Kramer. Symmetry-breaking Hopf bifurcation in anisotropic systems. Physica D **61**, 260 (1992).

[33] F. Ziebert and W. Zimmermann. Nonlinear analysis of oscillatory and demixing instabilities in filament-motor systems. (in preparation 2006).

[34] C. W. Gardiner. *Handbook of Stochastic Methods*, (Springer, Berlin, 1985).

[35] D. Smith, F. Ziebert, D. Humphrey, C. Duggan, W. Zimmermann and J. Käs. Molecular motors in cells: A rapid switch of biopolymer organization. (in preparation 2006)